PHASE TRANSITIONS IN SELF-ASSEMBLED MONOLAYERS OF ALKANETHIOLS CONTAINING THE POLAR GROUP

*Y. V. Sukhinin**

L. V. Kirensky Institute of Physics Russian Academy of Sciences
660036, Krasnoyarsk, Russia

Equilibrium states of the system of self-assembled monolayers (SAMs) of n-alkanethiol molecules $HS(CH_2)_{n-1}(X)$ with polar group X chemiabsorbed on the Au(111) crystal surface are considered. The couplings between the atoms (C, H) of the n-alkanethiols are approximated by the Lennard-Jones potential. The couplings between the n-alkanethiols and the crystal surface are approximated by the 12-3 potential. The interactions of polar groups and the self-images with the metal substrate are taken into consideration. The temperatures of the phase transitions, the structural order and equilibrium tilt, twist and azimuthal angles of the macromolecules, which depend on the dipole moments, are found.

1. INTRODUCTION

The self-assembled monolayers (SAMs) are a comparatively new type of organic monolayers [1–3], which are formed by spontaneous chemisorption of long-chain molecules from a solution to many different solid substrates (e.g., Au, Ag, Cu, Al, GaAs, Si). The self-assembled monolayers are presently the focus of considerable attention for technological and fundamental reasons. They have potential applications in such areas as corrosion prevention, wear protection, sensing devices, and the formation of well-defined microstructures [1, 4, 5]. They also present an excellent opportunity for the study of two-dimensional, condensed, organic solids at the microscopic level. Chemisorption of the thiol headgroup to the surface results in a long-range translational and orientational lattice structures. The monolayers are stable and have been studied extensively by transmission electron spectroscopy [6–9], optical ellipsometry [10–12], infrared spectroscopy [13, 14], electrochemistry [15, 16], and helium diffraction [17, 18]. These monolayers form at a fixed surface density, which remains nearly constant with changing temperature. This fact simplifies the study of rotational and conformational states of SAMs.

The most thoroughly studied and robust SAM system is $CH_3(CH_2)_{n-1}SH$ adsorbed on the Au(111) crystal surface. Theoretical investigations of its properties have given important insight into the nature of the long-range orderings of SAMs. To the extent possible, phenomenological approaches [19, 20], molecular dynamic (MD) simulations [21–26], and a model of the SAMs as the two-dimensional Ising model [27, 28] have explained the ground state structure and thermal-equilibrium orientational states of the SAM. One of the nearest problems is to study SAMs with more complex molecular chains, namely, self-assembled monolayers of alkanetiols containing a polar group. Molecular dynamic simulations of Langmuir–Blodgett monolayer with dipole group have already been considered [29, 30]. However, these simulations based
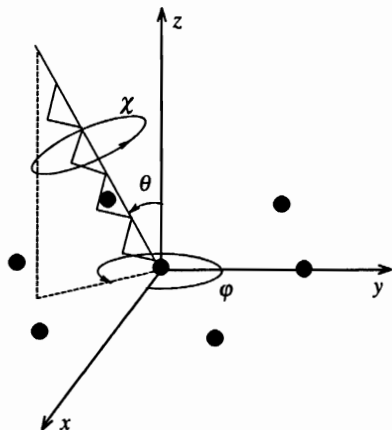
---

* E-mail: zeos@zeos.krascience.rssi.ru

Fig. 1. θ is the tilt angle of the molecule, χ is the chain twist (rotation) angle, and φ characterizes the tilt direction along the surface plane

on the so-called united atom model, which treats CH_2 groups as single interaction sites, and allowance for the packing patterns of alkyl chains with one or two molecules per unit cell give rise to an incorrect monolayer structure, the tilt angle, and tilt direction for zero dipole moment.

In this paper we are considering the effect of incorporating the polar group into self-assembled alkanethiol monolayers on the phase transitions and the molecular structure of the phases. We use an all-atoms model for hydrocarbon chains interactions. In order to avoid gauche or kink defect in alkyl chains we placed the polar group at the end of the chains.

2. MOLECULAR MODEL

The model describes the n-alkanethiol rigid chains terminating polar group. The SH headgroups of the alkanethiols form a $(\sqrt{3} \times \sqrt{3})R30°$ triangular lattice to adjust with (coordinate) Au(111) substrate. An all-atoms model includes hydrogen connected by rigid-bond couplings. This model is mainly based on the molecular model accepted by Hautman and Klein [22, 23] and Mar and Klein [24] except interactions between the chains. The chain has a zig-zag form and consists of hydrocarbon groups CH_2, beginning with sulfur and terminated by a polar group that a dipole moment **d** directs along the chain axis. We suppouse that arbitrary dipole moment belong to the molecular group CH_3. Hydrocarbon groups CH_2 and CH_3 are represented by single interaction sites including hydrogens. We assume that the chain may freely rotate about the chain axis as a whole with the twisting angle as the dihedral angle between the plane consisting of the normal to the gold surface, and the chain axis and plane defined by trans segments of the zig-zag molecular chain. Moreover, we assume that the chain may rotate relative to the crystal surface in such a way that the sulfur does not take part in this rotation. This rotation is determined by two angles: the tilting angle θ and the tilt direction φ (the precession angle of the long molecular axis about the surface normal to the gold crystal surface) (Fig. 1).

Following Ref. [27], let us consider the Lennard-Jones interactions between the atoms H, C, and S

$$U(R) = 4\epsilon \left[\left(\frac{\sigma}{R} \right)^{12} - \left(\frac{\sigma}{R} \right)^{6} \right]. \tag{1}$$

209

The Lennard-Jones (LJ) parameters ϵ and σ were chosen by fitting the potentials (1) to the Van der Waals (VdW) potential $\exp(-r^{-6})$ in such away that the potentials would have the same position, depth, and second derivatives at the point of minimum of the potentials. These parameters are listed in Tables 1 and 2. We used the LJ potential since the VdW potential has a negative divergence for small distances, which means that all chains will have a tendency to collapse on each other.

Table 1

Parameters of the Van der Waals potential $A\exp(-Br) - C/r^6$

A, 10^7 K			B, $\mathring{A}^{-1}$			C, K $\mathring{A}^6$			Refs.
A_{HH}	A_{HC}	A_{CC}	B_{HH}	B_{HC}	B_{CC}	C_{HH}	C_{HC}	C_{CC}	
0.33	1.4	6.0	4.08	4.08	3.08	2.5	6.3	16	[31]
1.50	1.5	1.5	5.00	4.13	3.42	2.2	7.0	21	[32]
1.10	1.1	1.1	4.64	3.94	3.42	2.7	7.2	17	[33]
0.92	1.1	1.3	4.64	3.94	3.42	2.2	6.9	19	[34]
0.46	6.8	2.1	4.54	4.56	3.58	2.1	6.4	20	[35]

Table 2

The Lennard-Jones coupling parameters

ϵ_{HH}, K	ϵ_{HC}, K	ϵ_{CC}, K	$\sigma_{0,HH}$, $\mathring{A}$	$\sigma_{0,HC}$, $\mathring{A}$	$\sigma_{0,CC}$, $\mathring{A}$	Refs.
18	29	52	2.653	2.903	3.118	[31]
36	38	36	2.338	2.814	3.418	[32]
30	30	30	2.498	2.939	3.387	[33]
24	29	34	2.500	2.939	3.387	[34]
33	30	920	2.316	2.941	1.842	[35]

Following Hautman and Klein [22], the interaction of the hydrocarbon groups CH_2 and CH_3 with the Au substrate was modeled by the 12-3 potential

$$V(z) = \frac{C_{12}}{(z - z_0)^{12}} - \frac{C_3}{(z - z_0)^3},\tag{2}$$

where $C_{12} = 2.8 \times 10^7$ K $\mathring{A}^{12}$, $C_3 = 17100$ K $\mathring{A}^3$, and $z_0 = 0.86$ $\mathring{A}$.

The dipole-dipole coupling of the dipoles $\mathbf{d}_i$ and $\mathbf{d}_j$ is

$$W(\mathbf{R}_{ij}) = \sum_{\alpha,\beta} W_{ij}^{\alpha,\beta} d_i^\alpha d_j^\beta,\tag{3}$$

where

$$W_{ij}^{\alpha,\beta} = \frac{\delta_{\alpha,\beta}}{R_{ij}^3} - \frac{3R_{ij}^\alpha R_{ij}^\beta}{R_{ij}^5},\tag{4}$$

and $\mathbf{R}_{ij}$ is the vector between the dipole moments; the magnitude of a dipole moment is measured in units of $1D = 4.8 \times 10^{-18}$ CGSE·cm.
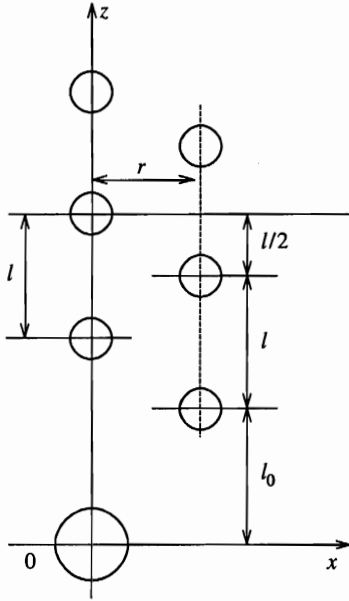
Fig. 2. Coordinates defining the model of the zig-zag n-thiol chain chemisorbed to a gold substrate; $l_0 = 1.58$ Å, $l = 2.506$ Å, $r = 0.878$ Å, $h = 1.04$ Å, $\alpha = 55°$

The coordinates of the kth carbons in the local coordinate system with $\theta = 0$, $\varphi = 0$, and $\chi = 0$ for the zig-zag chain in Fig. 2 are

$$\mathbf{R}_{Ck} = \begin{cases} (r, & 0, & l_0 + (k-1)l/2), & k = 1, 3, 5, ..., \\ (0, & 0, & l_0 + (k-1)l/2), & k = 2, 4, 6, ..., \end{cases} \tag{5}$$

where the distances in the chain are shown in Fig. 2, and χ is the twisting angle. The coordinates of the hydrogen are

$$\mathbf{R}_{Hks} = \begin{cases} (r + h\cos\alpha, & hs\sin\alpha, & l_0 + (k-1)l/2), & k = 1, 3, 5, ..., \\ (-h\cos\alpha, & hs\sin\alpha, & l_0 + (k-1)l/2), & k = 2, 4, 6, ... \end{cases} \tag{6}$$

The coordinates of the dipole are the same as those C_n.

In order to find the coordinates defining the carbon and hydrogen atoms of the n-thiol chain in the coordinate system of the substrate, it is necessary to use the transformations of rotations determined by the Euler matrix

$$\mathbf{T}(\varphi, \theta, \chi) = \begin{pmatrix} \cos\varphi & -\sin\varphi & 0 \\ \sin\varphi & \cos\varphi & 0 \\ 0 & 0 & 1 \end{pmatrix} \begin{pmatrix} \cos\theta & 0 & \sin\theta \\ 0 & 1 & 0 \\ -\sin\theta & 0 & \cos\theta \end{pmatrix} \begin{pmatrix} \cos\chi & -\sin\chi & 0 \\ \sin\chi & \cos\chi & 0 \\ 0 & 0 & 1 \end{pmatrix}.$$

This gives a transformation

$$\mathbf{R}(\varphi, \theta, \chi) = \mathbf{T}(\varphi, \theta, \chi)\mathbf{R}. \tag{7}$$

Experimental data [8, 9] show that the chain is tilted to the next nearest neighbour (NNN) in a direction from the NNN direction ($\varphi \sim 10°$). Below we consider the tilted phase ($\theta > 0$) only. A number and equilibrium angular positions of the chains of the paraphase depended on
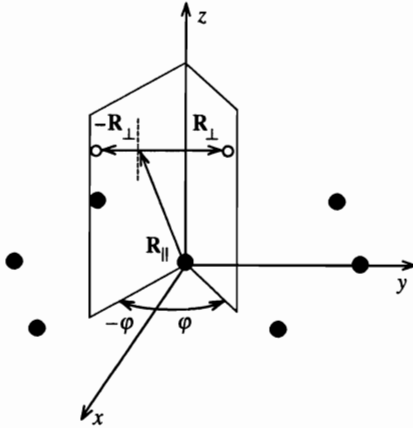
Fig. 3. Symmetrical positions of an atom of the n-thiol chains in the tilted phase

the symmetry of the system. One can see that the one-body potential of the chain-S (1) and the chain-Au (2) is four fold degenerate with respect to the angular positions of a chain $R(\varphi, \theta, \chi)$, $R(-\varphi, \theta, -\chi)$, $R(\pi + \varphi, \theta, \chi)$, $R(\pi - \varphi, \theta, -\chi)$. If one takes into account the contribution in the potential of the chain from the straight chain of carbon atoms [in (5) $r = 0$], then the chain-chain interactions (1) remove the mirror symmetry in the yz plane. Hence, the total one-body potential of a chain is two fold degenerate with respect to the angular positions $R(\varphi, \theta, \chi)$ and $R(-\varphi, \theta, -\chi)$. This degeneracy was shown quantitatively in Ref. [27]. The equilibrium state of the chains $R(\varphi_0, \theta_0, \chi_0)$ and that of the mirror plane xz $R(-\varphi_0, \theta_0, -\chi_0)$ is found from the minimum thermodynamic potential for $T > T_c$ and defined below.

In order to consider the phase transition with spontaneous breakdown of the symmetry we follow Vaks [36] and write the following expressions for the rotated coordinates of the atoms:

$$R_s = R(s\varphi, \theta, s\chi) = \frac{1}{2}[T(\varphi, \theta, \chi)R + T(-\varphi, \theta, -\chi)R] +$$

$$+ s\frac{1}{2}[T(\varphi, \theta, \chi)R - T(-\varphi, \theta, -\chi)R] = R_{\|} + sR_{\perp}, \quad s = \pm 1. \tag{8}$$

Obviously, since $R_{\|} = (R_{+1} + R_{-1})/2$, $R_{\perp} = (R_{+1} - R_{-1})/2$ and $|R_{+1}| = |R_{-1}|$,

$$R_{\|}R_{\perp} = 0,$$

and $R_{\perp}$ is directed along the y axis, as shown in Fig. 3. As the basis vectors of the two-dimensional triangular lattice of sulfur atoms we chose the vectors

$$a_1 = a(\sqrt{3}/2, 1/2, 0), \quad a_2 = a(0, 1, 0), \tag{9}$$

where the lattice constant $a = 4.97$ Å. Now let us specify the coordinates of the atoms of the jth chain on the surface:

$$R_{jgk} = R_j + R_{\|,gk} + s_j R_{\perp,gk}, \tag{10}$$

where j runs over all sites of the triangular lattice, k runs over the atomic groups CH_2 and CH_3 along the chain, and g runs over the specific atomic groups ($g = C, H_1$, and H_2). Accordingly, the dipole moment of the jth chain is

$$d_j = d_{\|} + s_j d_{\perp}, \tag{11}$$

where $\mathbf{d}_\perp \| y$, and $\mathbf{d}_\| \mathbf{d}_\perp = 0$.

Substituting expressions (8) and (10) into the potential interactions (1) and (2), we obtain the following expression for the LJ coupling chain-chain energy:

$$\frac{1}{2} \sum_{i,j} \sum_{g,g'} \sum_{k,k'} U_{gg'}(\mathbf{R}_{ij} + \mathbf{R}_{0,gk} - \mathbf{R}_{0,g'k'} + s_i \mathbf{R}_{1,gk} - s_j \mathbf{R}_{1,g'k'}), \tag{12}$$

where $\mathbf{R}_{ij} = \mathbf{R}_i - \mathbf{R}_j$, and for the total chain-surface energy, which includes a coupling of the n-thiol atoms (C, H) with the sulfur atoms,

$$\sum_i \sum_g \sum_k V(R^z_{0,k} + s_i R^z_{1,k}) + \sum_{i,j} \sum_g \sum_{k,k'} U_{g\mathrm{S}}(\mathbf{R}_{ij} + \mathbf{R}_{0,gk} + s_i \mathbf{R}_{1,gk}). \tag{13}$$

In accordance with Eq. (1), we introduce the notation

$$U_{g,g'} = 4\epsilon_{g,g'} \left[\left(\frac{\sigma_{g,g'}}{R} \right)^{12} - \left(\frac{\sigma_{g,g'}}{R} \right)^6 \right], \tag{14}$$

and the notation $U_{g\mathrm{S}}$ means the interaction of the chain's atoms with the sulfur.

A single dipole spaced apart from a metal feels an interaction with its self-image, so a dipole-dipole part of the chain-chain energy consists of dipole-dipole, dipole-image and image-image interactions. Substituting expressions (9) and (10) into (3), we obtain the energy of the dipole-dipole coupling

$$\sum_{i,j} \left[W(\mathbf{R}_{ij} + (s_i - s_j)\mathbf{R}_{\perp,C_n}) + \frac{1}{2} W(\mathbf{R}_{ij} + \mathbf{Z}_{12} + (s_i - s_j)\mathbf{R}_{\perp,C_n}) \right], \tag{15}$$

where $\mathbf{Z}_{12}$ is the vector between the real dipole and its self-image.

In order to simplify expressions (12), (13), and (15) we introduce the projection operators $s^\pm = (1 \pm s)/2$. Then for any function f of the two operators s_1 and s_2 there is an identity [36]

$$\begin{aligned} f(xs_1 + ys_2) &= (s_1^+ + s_1^-)(s_2^+ + s_2^-)f(xs_1 + ys_2) = \\ &= s_1^+ s_2^+ f(x+y) + s_1^+ s_2^- f(x-y) + s_1^- s_2^+ f(-x+y) + s_1^- s_2^- f(-x-y). \end{aligned} \tag{16}$$

Using this identity, we can write the following expression for the total energy of the SAM:

$$E = E_0 - \frac{1}{2} \sum_{ij} J_{ij}(\theta, \varphi, \chi) s_i s_j. \tag{17}$$

In accordance with Eq. (16), we obtain the expressions

$$E_0 = \frac{1}{4} \sum_{ij} \sum_{s,s'} (U^{ij}_{s,s'} + W^{ij}_{s,s'}) + \frac{1}{2} \sum_i \sum_s V^i_s, \tag{18}$$

$$J_{ij} = \frac{1}{4} \sum_{s,s'} ss' U^{ij}_{s,s'} + \frac{1}{4} \sum_{s,s'} ss' W^{ij}_{s,s'}, \tag{19}$$

where

$$U^{ij}_{s,s'} = \frac{1}{2} \sum_{gg'} \sum_{kk'} U_{gg'}(\mathbf{R}_{ij} + \mathbf{R}_{\|,gk} - \mathbf{R}_{\|,g'k'} + s\mathbf{R}_{\perp,gk} - s'\mathbf{R}_{\perp,g'k'}),$$

213

$$W_{s,s'}^{ij} = W(\mathbf{R}_{ij} + (s - s')\mathbf{R}_{\perp,c_n}) + \frac{1}{2}W(\mathbf{R}_{ij} + \mathbf{Z}_{12} + (s - s')\mathbf{R}_{\perp,c_n}), \tag{20}$$

$$V_s^i = \sum_g \sum_k V(R_{\parallel,k}^z + sR_{\perp,k}^z) + \sum_j \sum_g \sum_k U_{gs}(\mathbf{R}_{ij} + \mathbf{R}_{\parallel,gk} + s\mathbf{R}_{\perp,gk}).$$

The linear term $\sum_i B_i s_i$ is absent in Eq. (17) due to the symmetry.

3. MEAN-FIELD APPROXIMATION

According to (17), the thermodynamic potential of the SAM is

$$F = E_0(\theta, \varphi, \chi) - T \ln \mathrm{Sp}_{\{s_i\}} \exp\left[\frac{1}{2}\sum_{ij} J_{ij}(\theta, \varphi, \chi)\frac{s_i s_j}{T}\right]. \tag{21}$$

A mean-field approximation of Eq. (21) is given by the expression [36]

$$F = E_0(\theta, \varphi, \chi) + \frac{1}{2}\sum_{ij} J_{ij}(\theta, \varphi, \chi)\langle s_i\rangle\langle s_j\rangle -$$

$$- T\sum_i \ln\left[2\,\mathrm{ch}\left(\sum_j J_{ij}(\theta, \varphi, \chi)\frac{\langle s_j\rangle}{T}\right)\right]. \tag{22}$$

One can see from Eq. (22) that in the paraphase ($\langle s_i\rangle = 0$) the minimum $E_0(\varphi, \theta, \chi)$ with respect to the angles gives equilibrium $\varphi_0, \theta_0, \chi_0$ SAM's chains. The order parameter $\langle s_i\rangle \neq 0$ is defined as a solution of the state equations of state [37]

$$\langle s_i\rangle = \mathrm{th}\left[\sum_j J_{ij}(\theta, \varphi, \chi)\frac{\langle s_j\rangle}{T}\right]. \tag{23}$$

A substitution of solutions of this equation into (22) and self-consistent minimization of the thermodynamic potential over three angles give the complete equilibrium state of the SAM. Next, according to Eq.(23), the structure ordered phase is determined by the wave vector $\mathbf{q}_0$, for which

$$J_{\mathbf{q}} = \sum_j J_{ij} \exp(i\mathbf{q}\mathbf{R}_{ij}) \tag{24}$$

takes on the maximum value and $T_c = J_{\mathbf{q}_0}$ [37].

The first item transform of (19) under near neighboring chain-chain coupling is given by the expression [27]

$$U(\mathbf{q}) = 2J_1 \cos(2\pi\xi_1) + 2J_1 \cos\left[2\pi(\xi_1 - \xi_2)\right] + 2J_2 \cos(2\pi\xi_2), \tag{25}$$

where the wave vector $\mathbf{q} = \xi_1\mathbf{b}_1 + \xi_2\mathbf{b}_2$ is written about the basis reciprocal to (9)

$$\mathbf{b}_1 = 4\pi a^{-1}\left(1/\sqrt{3}, 0, 0\right), \quad \mathbf{b}_2 = 2\pi a^{-1}\left(-1/\sqrt{3}, 1, 0\right), \tag{26}$$
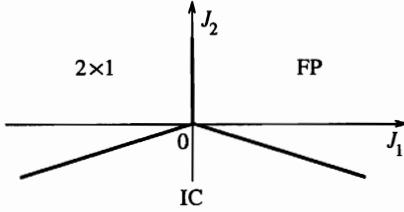
Fig. 4. Phase diagram of the Ising model on the triangular lattice

J_1 is the coupling constant along the vectors $\pm\mathbf{a}_1$, $\pm(\mathbf{a}_2 - \mathbf{a}_1)$, and J_2 is the coupling constant along the vectors $\pm\mathbf{a}_2$.

One points to fact that as $\mathbf{d} = 0$ expression (24) is reduced to (25), maximums which give the following structure ordered phase and the transition temperature [27]:

$$1) \quad \xi_1 = 0, \quad \xi_2 = 0, \quad T_c = 4J_1 + 2J_2 \quad \text{(ferro)};$$

$$2) \quad \xi_1 = 0.5, \quad \xi_2 = 0, \quad T_c = -4J_1 + 2J_2 \quad (2 \times 1); \qquad (27)$$

$$3) \quad \xi_1 = 0.5\xi_2, \quad T_c = -\frac{J_1^2}{J_2} - 2J_2, \quad \left|\frac{J_1}{2J_2}\right| \le 1 \quad \text{(IC)}.$$

The phase diagram, which corresponds to Eq. (27), is shown in Fig. 4.

The dipole-dipole interaction transform of (19) is computed by Ewald's method [38], fitting to the $2D$ lattice. Formally, the Fourier transform (4) can be found as follows:

$$W_{q,x}^{\alpha,\beta} = -\frac{\partial^2}{\partial x_\alpha \partial x_\beta} \sum_l \frac{e^{iql}}{|l - x|}, \qquad (28)$$

where $l = l_1\mathbf{a}_1 + l_2\mathbf{a}_2, l_1, l_2$ is an integer, and $\mathbf{a}_1$ and $\mathbf{a}_2$ defined by expressions (9). After the fashion of Ewald the series of (28) for a plane lattice is presented by the sum of two series:

$$\sum_l \frac{e^{iql}}{|l - x|} = \sum_l \frac{\text{erfc}(R|l - x|)}{|l - x|} +$$

$$+ \frac{\pi}{S_0} \sum_g \frac{e^{ix(q+g)}}{|g+q|} \left[e^{z|q+g|} \text{erfc}\left(\frac{|q+g|}{2R} + zR\right) + e^{-z|q+g|} \text{erfc}\left(\frac{|q+g|}{2R} - zR\right) \right], \quad (29)$$

where

$$\text{erfc}(x) = \frac{2}{\sqrt{\pi}} \int_x^\infty e^{-y^2} dy,$$

$\mathbf{g} = g_1\mathbf{b}_1 + g_2\mathbf{b}_2$, g_1, g_2 is an integer, $\mathbf{b}_1$ and $\mathbf{b}_2$ are defined by expressions (26), S_0 is the unit cell area, z is the component along the z axis of the vector $\mathbf{x}$, and R is the adjustable parameter of the velocity convergence of the series. Note that Eq. (29) was obtained in Ref. [29] for $q = 0$.

The results of self-consistent numerical minimization procedure of (22) are given in Figs. 5–8 and Table 3. The first feature of the temperature transition is high sensitivity to the choice of the coupling constants listed in Table 2. For the choice of the coupling constants defined in Refs. [32, 35] there is ordered phase sequence from the ferro or 2×1 to the IC (Figs. 6 and 8). However, for the choice of coupling constants defined in Refs. [31, 33, 34] there is IC phase (Table 3), where the transition temperature T_c increase with increasing dipole moment.
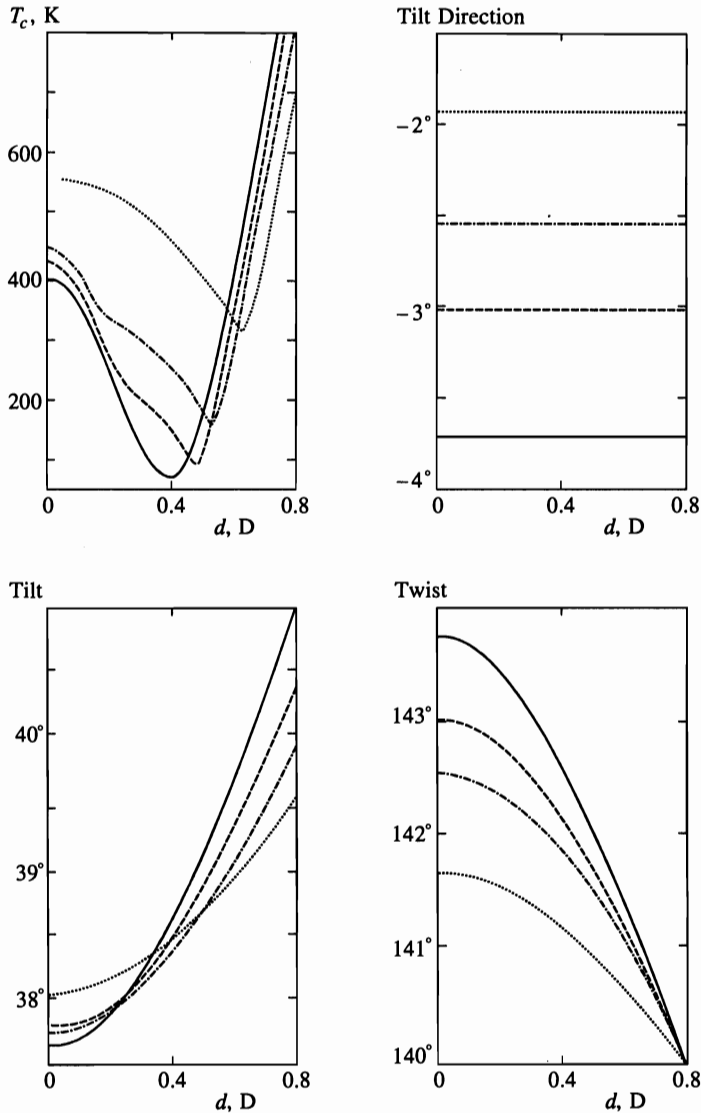
Fig. 5. Curves of the temperature transition T_c and the equilibrium angles of the n-thiols, plotted as functions of the dipole moment, are described by the solid ($n = 8$), dashed ($n = 10$), dot-dashed ($n = 12$), and dotted ($n = 17$) lines for the coupling parameters from Ref. [32]

4. DISCUSSION AND CONCLUSIONS

An advantage of using the Ising variable is that a rich variety of the couplings between atoms of the n-thiols and the couplings with the crystal surface is reduced to a few competing exchange parameters. For $d = 0$ it allow one to establishing a simple phase diagram of the system shown in Fig. 4. The SAMs are described by the Ising model on the triangular lattice with exact solution [39]. Ferro, 2×1 and incommensurate phases are the only possible ordered
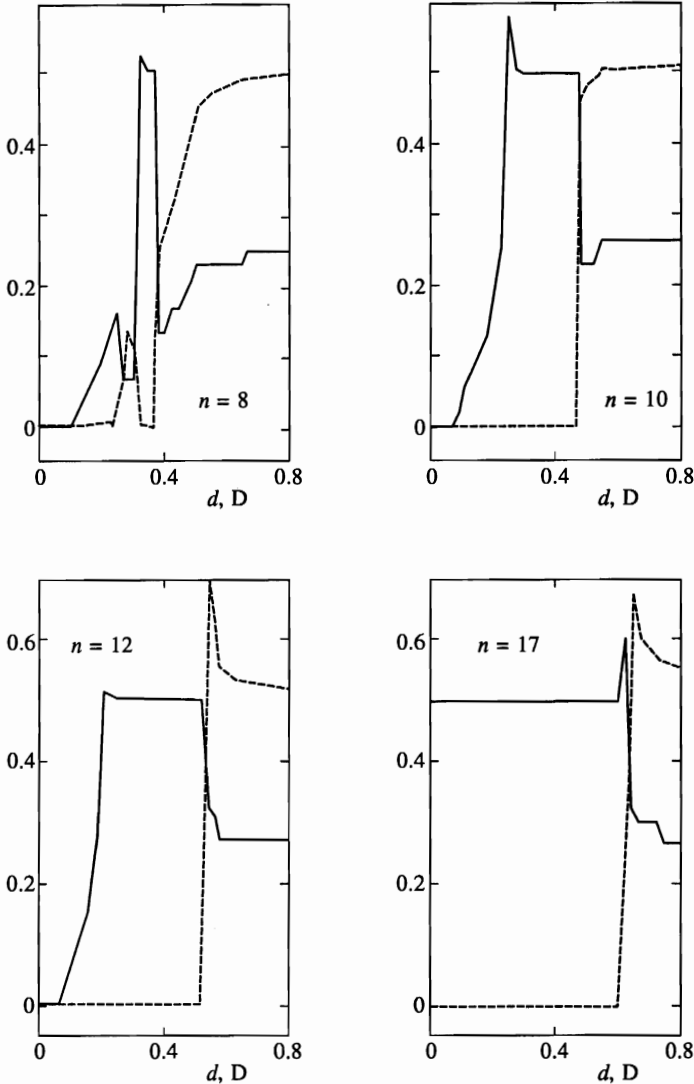
Fig. 6.   The components of the wave vector of the ordered structure ξ_1 (solid) and ξ_2 (dashed) for the coupling parameters from Ref. [32]

states of the system of the n-thiols which are self-assembled on the crystal surface Au(111). For $d \neq 0$ competition a LJ interaction and a dipole-dipole coupling can give rise to various combinations of the structures.

The most interesting behavior of the critical temperature and a sequence of ordered structures upon change in the dipole moment has been found for the LJ's parameters from Refs. [32, 35]. The transition temperature dependence is that T_c with $d \neq 0$ can be smaller one with $d = 0$. In particular, the lowest temperature of the phase transition is realized for the parameters taken from Refs. [32, 34]. T_c is quite sensitive to the coupling parameters which change many times. Moreover, it is necessary to take into consideration that all coupling
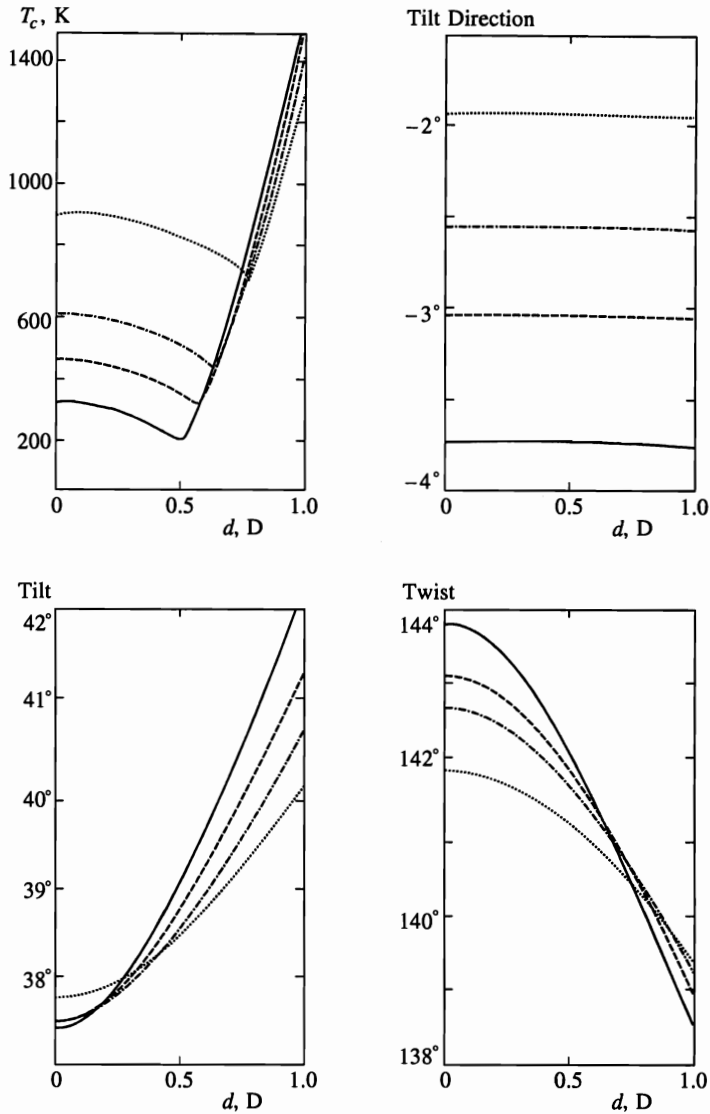
Fig. 7. The same as in Fig. 5 for Ref. [35]

parameters listed in Table 1 are given for the case of three-dimensional crystals in which the distances between the atomic groups CH_2 may differ in comparison with the case of the SAM. Therefore, the coupling constants listed in Tables 1 and 2 should be considered carefully. As far as the structure of the ordered phase for any set coupling parameters is concerned, with increasing dipole moment the incommensurate phase is described by the modulation vector either near $\xi = (0.25, 0.5)$ or near $\xi = (0.3, 0.6)$.

The phase transition leads to a freezing of the jumps of the chains between two fold degenerated states with equilibrium azimutal and twist angles φ_0, χ_0 is given in Figs. 5 and 7
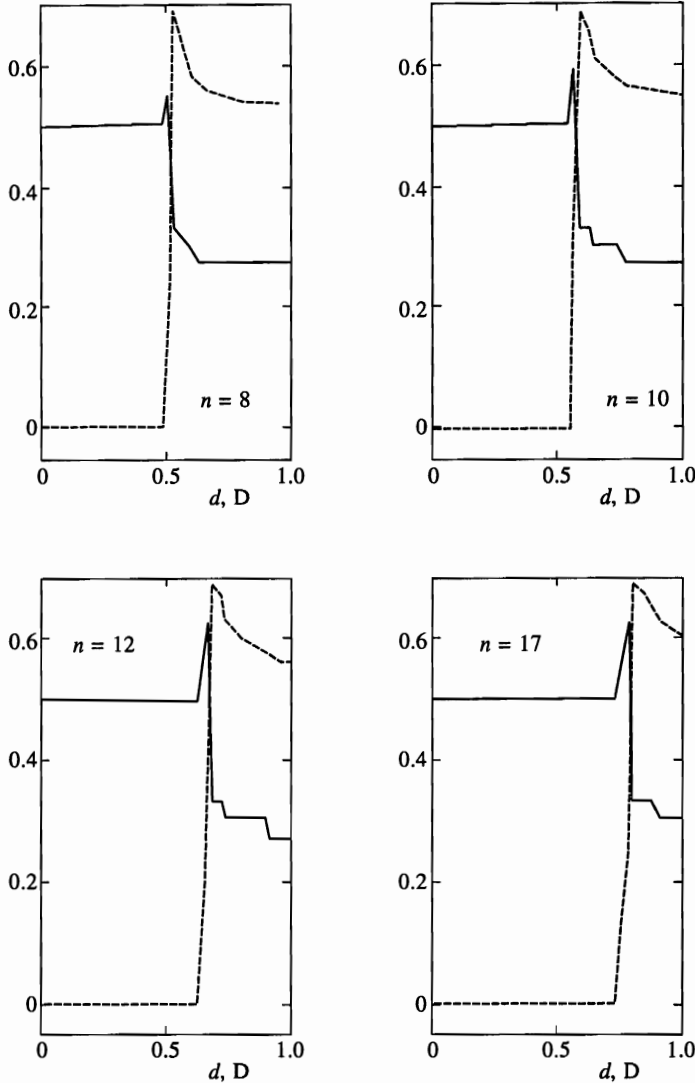
Fig. 8. The same as in Fig. 6 for Ref. [35]

and Table 3 for various references. The values of these angles agree with the experimental observations and theoretical considerations except for the azimutal angle which was found experimentally to be $\varphi \sim 10°$ for $d = 0$ and $10 < n < 20$ (Ref. [9]).

The final feature of the phase transition to the twisted ordered phase is that it is a first-order transition. The reason is analogous to the effect of elastic media on the order of the phase transition [36, 40], where the spontaneous ordering gives rise to a distortion of the crystal which in turn leads to a slight increase in the exchange integrals. Hence, the Curie temperature from the paraphase turns out to be lower than the Curie temperature from the ordered phase. Similarly, in the system of the n-thiol's chains a spontaneous twist ordering of the chains give

219

Table 3

The critical temperatures, the wave vector, and the equilibrium angles

n	T_c, K	ξ_1	ξ_2	θ_0	χ_0	φ_0	Refs.
				$d = 0.5$ D			
8	1249.6	0.259	0.517	−3.88	35.55	143.75	[31]
12	1701.6	0.259	0.525	−2.68	35.11	142.95	"
16	2156.9	0.259	0.529	−2.05	34.90	142.50	"
8	688.5	0.259	0.520	−3.82	36.21	143.75	[33]
12	855.6	0.273	0.538	−2.64	35.80	143.00	"
16	1028.7	0.273	0.549	−2.02	35.61	142.58	"
8	619.7	0.259	0.525	−3.81	36.68	143.37	[34]
12	745.3	0.273	0.546	−2.63	36.23	142.69	"
16	878.0	0.273	0.561	−2.01	36.01	142.30	"
				$d = 1.0$ D			
8	2857.1	0.253	0.510	−3.79	38.34	141.53	[31]
12	3224.2	0.259	0.519	−2.63	37.04	141.61	"
16	3642.2	0.259	0.524	−2.02	36.39	141.55	"
8	2227.0	0.253	0.512	−3.77	39.05	141.19	[33]
12	2311.7	0.267	0.524	−2.60	37.72	141.44	"
16	2442.9	0.267	0.532	−1.99	37.08	141.46	"
8	2154.5	0.267	0.516	−3.77	39.71	140.52	[34]
12	2200.6	0.267	0.528	−2.60	38.29	140.91	"
16	2290.4	0.267	0.537	−1.99	37.59	141.01	"

rise to a change in the tilt. This in turn leads to a change of the exchange integrals defined by Eq. (19).

References

1. J. D. Swalen, D. L. Allara, J. D. Andrade et al., Langmuir **3**, 932 (1987).
2. L. H. Dubois and R. G. Nuzzo, Ann. Rev. Phys. Chem. **43**, 437 (1992).
3. R. G. Nuzzo, F. A. Fusco, and D. L. Allara, J. Amer. Chem. Soc. **109**, 2358 (1987).
4. P. E. Laibinis and G. M. Whitesides, J. Amer. Chem. Soc. **114**, 9022 (1992).
5. A. Kumar, H. A. Biebuyck, and G. M. Whitesides, Langmuir **10**, 1498 (1994).
6. L. S. Strong and G. M. Whitesides, Langmuir **4**, 546 (1988).
7. C. E. D. Chidsey and D. N. Loiacono, Langmuir **6**, 682 (1990).
8. P. Fenter, P. Eisenberger, and K. S. Liang, Phys. Rev. Lett. **70**, 2447 (1993).

9. P. Fenter, P. Eisenberger, K. S. Liang, and A. Eberhard, J. Chem. Phys. **106**, 1600 (1997).

10. C. D. Bain, E. B. Troughton, Y.-T. Tao et al., J. Amer. Chem. Soc. **111**, 321 (1989).

11. G. M. Whitesides and P. E. Laibinis, Langmuir **6**, 87 (1990).

12. S. D. Evans, E. Urankar, A. Ulman, and N. Ferris, J. Amer. Chem. Soc. **113**, 4121 (1991).

13. R. G. Nuzzo, L. H. Dubois, and D. L. Allara, J. Amer. Chem. Soc. **112**, 558 (1990).

14. R. G. Nuzzo, E. M. Korenic, and L. H. Dubois, J. Chem. Phys. **93**, 767 (1990).

15. T. T. T. Li and M. J. Weaver, J. Amer. Chem. Soc. **106**, 6107 (1984).

16. M. D. Porter, T. B. Bright, D. L. Allara et al., J. Amer. Chem. Soc. **109**, 3559 (1987).

17. N. Camillone III, C. E. D. Chidsey, G. Liu et al., J. Chem. Phys. **94**, 8493 (1991).

18. N. Camillone III, C. E. D. Chidsey, G. Liu et al., J. Chem. Phys. **98**, 3503 (1993).

19. R. Nagarajan and E. Ruckenstein, Langmuir **7**, 2934 (1991).

20. V. M. Kaganer, M. A. Osipov, and I. R. Peterson, J. Chem. Phys. **98**, 3512 (1993).

21. C. M. Knobler and R. C. Desai, Ann. Rev. Phys. Chem. **43**, 207 (1992).

22. J. Hautman and M. L. Klein, J. Chem. Phys. **91**, 4994 (1989).

23. J. Hautman and M. L. Klein, J. Chem. Phys. **93**, 7483 (1990).

24. W. Mar and M. L. Klein, Langmuir **10**, 188 (1994).

25. S. Shin, N. Collazo, and S. A. Rice, J. Chem. Phys. **98**, 3469 (1993).

26. M. A. Moller, D. J. Tildesley, K. S. Kim et al., J. Chem. Phys. **94**, 8390 (1991).

27. A. F. Sadreev and Y. V. Sukhinin, Phys. Rev. B **54**, 17966 (1996).

28. A. F. Sadreev and Y. V. Sukhinin, J. Chem. Phys. **107**, 2643 (1997).

29. V. V. Kislov, Y. A. Kriksin, and I. V. Taranov, Radiotechnika i Elektronika **38**, 539 (1993).

30. V. V. Kislov, Y. A. Kriksin, and I. V. Taranov, Radiotechnika i Elektronika **41**, 241 (1996).

31. L. S. Bartell, J. Chem. Phys. **32**, 827 (1960).

32. A. I. Kitaigorodsky, Tetrahedron **14**, 230 (1961).

33. A. I. Kitaigorodsky, *Molecular Crystals and Molecules*, Academic Press, New York and London (1973), Chap. 2.

34. A. I. Kitaigorodsky, Adv. Struct. Res. **3**, 204 (1970).

35. T. Wasiutyński and T. Luty, Acta Physica Polon. A **45**, 551 (1974).

36. V. G. Vaks, *Introduction to Microscopic Theory of Ferroelectrics*, Nauka, Moscow (1973) (in Russian).

37. R. Blinc and B. Žekš, *Soft Modes in Ferroelectrics and Antiferroelectrics*, North-Holland Publ., Amsterdam (1974).

38. J. M. Ziman, *Principels of the Theory of Solids, 2nd ed.*, Cambridge (1972).

39. R. J. Baxter, *Exactly Solved Models in Statistical Mechanics*, Academic Press, New York (1982), Chap. 11.

40. O. K. Rice, J. Chem. Phys. **22**, 1535 (1954).